ESTIMATION OF THE TIRE CORNERING STIFFNESS AND ITS APPLICATION TO ACTIVE CAR STEERING

Wolfgang Sienel
DLR, German Aerospace Research Center
Institute of Robotics and System Dynamics
Oberpfaffenhofen, 82234 Wessling, Germany
Email: Wolfgang.Sienel@dlr.de

KEYWORDS: Nonlinear tire characteristics, automobiles, active steering, robust decoupling

Abstract

Active steering systems can help the driver to master critical driving situations, for example aquaplaning and μ-split braking. In these situations it is likely that the tires reach their performance limits, where nonlinear effects like saturation play an important role. Tires are the part in vehicle dynamics afflicted with the highest degree of nonlinearity – due to saturation – and uncertainty – due to whether conditions. Therefore, active steering systems have to be designed considering the uncertain and nonlinear tire characteristics which are determined by the road-tire-contact.
This paper demonstrates how an important tire parameter, the cornering stiffness, can be estimated by measurement of dynamic vehicle parameters like lateral accelerations and yaw rate. This parameter indicates whether the saturation region of the tire is reached or not. Based on the estimate of the tire the robust decoupling control law by Ackermann [1] for active front steering is extended.

1 Introduction

Critical driving situations may be of rather different quality: Think for example of a child crossing unexpectedly the street and forcing the driver to an evasive action. Or imagine a ride on snow-covered road in winter. Though of different kind, the driver would like his car to react in both scenarios as under normal driving situations. Especially, the unexperienced driver only knows a limited subset of driving conditions and once caught in a new situation, easily overreacts and destabilizes the car.
Active car steering is a possible approach to enhance driving safety under critical situations. Control systems react much faster than human drivers. Figure 1 illustrates a block diagram of a vehicle equipped with active front steering. The front steering angle δ_f is composed of the driver commanded steering wheel angle δ_S and an additional controller commanded angle δ_c:

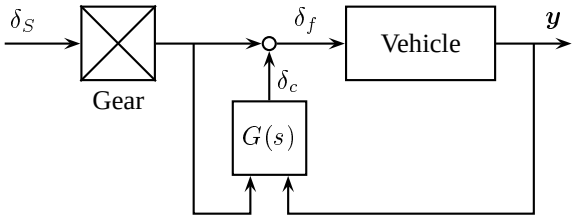

Figure 1: Block diagram of a vehicle with active front steering

$$\delta_f = i_S \cdot \delta_S + \delta_c \tag{1}$$

where i_S is the gear ratio. The control law $G(s)$ generally requires input of the driver commanded steering wheel angle as reference and measurement of dynamical variables, like yaw rate and lateral accelerations. The block diagram neglects the actuator which is necessary to set the additional front steering angle δ_c. Technical solutions for this purpose with a mechanical connection from steering wheel to the front tires can be found in the patent literature.

The task of active steering is to extend the region of the driver accustomed linear behavior of the vehicle as far as possible to the car's performance limits. The most crucial component of the vehicle dynamics limiting its range of linear behavior is the road-tire contact: the road condition may range from dry asphalt to ice-covered roads, the tire may be worn out or loose pressure rapidly. Other parameters like the load mass of passenger cars play a subdominant role. It is clear that the controller $G(s)$ has to be robust with respect to the huge uncertainty in the road-tire contact. Most approaches assume linearized models in the design phase and do not consider the nonlinearity in the tire characteristics. These approaches may yield good results as long as the vehicle remains within the linear region of the tire characteristics. However, the controller may even worsen the driving situation drastically compared to the conventional vehicle, as soon as the nonlinear region of the tire characteristics is entered.

An active front steering system based on robust decoupling was presented by Ackermann [1]: Unity feedback of the

yaw rate via an integrator robustly decouples the lateral acceleration at the front axle from the yaw motion:

$$\dot{\delta}_c = i_S F(v) \cdot \delta_S - r \tag{2}$$

i.e. the decoupling property is independent of velocity and mass. The velocity dependent gain $F(v)$ determines the stationary behavior of the vehicle.

Experiments with a test car showed good disturbance rejection of yaw torque disturbances for cross-wind excitation and μ-split braking maneuvers [2]. However, the inspected driving situations did not lead to large tire slip angles such that lateral tire nonlinearities did not play a role in these tests.

Robust decoupling also holds considering nonlinear tire dynamics [3], but the decoupling property by itself does not guarantee satisfying handling qualities or even stability. In the next section the vehicle dynamics will be investigated assuming a nonlinear tire model. In Section 3, it will be shown, how an important tire parameter, the cornering stiffness can be estimated and an extension of the control law (2) using this estimate concludes the paper.

2 Tire characteristics and vehicle properties

The tire is the component of vehicle dynamics afflicted with the most uncertainty. Figure 2 illustrates the lateral tire force in dependency of the tire side slip angle α for various road adhesion coefficients. The plots were produced using a HSRI model [4] assuming no longitudinal slip, i.e. freely spinning wheels.

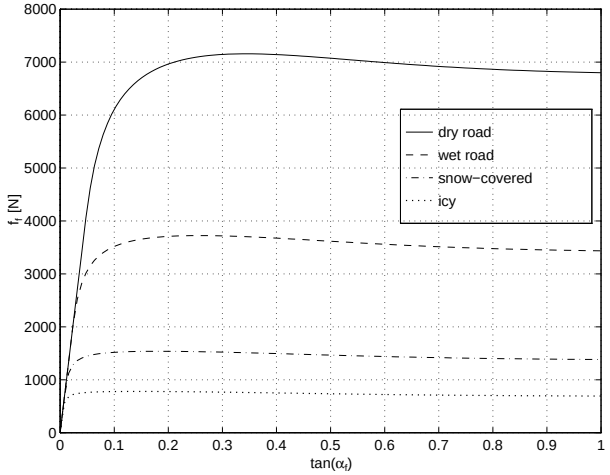

Figure 2: Tire characteristics for different road conditions at 50 km h^{-1} and a normal force of 8000 N (per axle)

For the investigations in this paper a nonlinear single track model is assumed. The single track model is obtained by lumping the two wheels of each axle into one wheel at the centerline of the vehicle, see Figure 3. The variables in Figure 3 denote

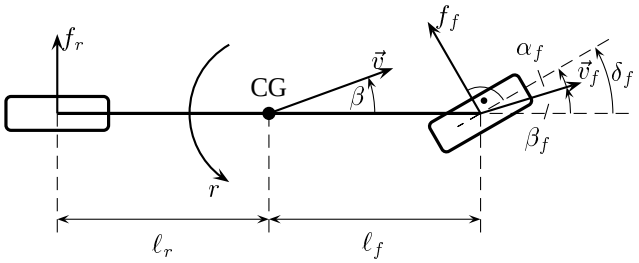

Figure 3: Sketch of the single track model

f	lateral tire force
ℓ	distance from center of gravity (CG) to axle
δ	steering angle
β	side slip angle
α	tire slip angle
$\vec{v}$	velocity vector, its magnitude is v
r	yaw rate

Here and throughout the paper the indices $._f$ and $._r$ refer to the front and rear axle, respectively, otherwise to the center of gravity.

The tire forces illustrated in Figure 2 can be projected onto longitudinal and lateral force f_x and f_y at CG and yaw torque m_z:

$$\begin{bmatrix} f_x \\ f_y \\ m_z \end{bmatrix} = \begin{bmatrix} -\sin\delta_f & 0 \\ \cos\delta_f & 1 \\ \ell_f \cos\delta_f & -\ell_r \end{bmatrix} \begin{bmatrix} f_f(\alpha_f) \\ f_r(\alpha_r) \end{bmatrix} \tag{3}$$

The dynamics of the vehicle are

$$\begin{bmatrix} mv(\dot{\beta}+r) \\ m\dot{v} \\ J\dot{r} \end{bmatrix} = \begin{bmatrix} -\sin\beta & \cos\beta & 0 \\ \cos\beta & \sin\beta & 0 \\ 0 & 0 & 1 \end{bmatrix} \begin{bmatrix} f_x \\ f_y \\ m_z \end{bmatrix} \tag{4}$$

where m denotes vehicle mass and J the yaw inertia. The dependencies of the tire variables are

$$\begin{aligned} \delta_f &= \alpha_f + \beta_f \\ 0 &= \alpha_r + \beta_r \end{aligned} \tag{5}$$

where the tire side slip angles can be expressed as

$$\begin{aligned} \tan\beta_f &= \tan\beta + \frac{\ell_f r}{v\cos\beta} \\ \tan\beta_r &= \tan\beta - \frac{\ell_r r}{v\cos\beta} \end{aligned} \tag{6}$$

The above equations can be found in the automotive literature or in [5]. In order to obtain the linearized version of the vehicle dynamics the equations (3), (4), and (6) are linearized, the velocity v is assumed constant, i.e. $\dot{v} \equiv 0$, and the linear tire model

$$\begin{aligned} f_f(\alpha_f) &= c_{f0} \cdot \alpha_f \\ f_r(\alpha_r) &= c_{r0} \cdot \alpha_r \end{aligned} \tag{7}$$

is used. The parameters c_{f0} and c_{r0} are the cornering stiffnesses of the tire obtained by linearizing the nonlinear tire characteristics of Figure 2 at the origin.

For the following investigations the more general definition

$$c_f(\alpha_f) = \frac{\mathrm{d}f_f(\alpha_f)}{\mathrm{d}\alpha_f} \tag{8}$$

for the cornering stiffness is assumed. A first order approximation

$$f_f(\alpha_f) = \left.\frac{\mathrm{d}f_f(\alpha_f)}{\mathrm{d}\alpha_f}\right|_{\alpha_f=\alpha_{f0}} \cdot \alpha_f + f_{f0}(\alpha_{f0}) \tag{9}$$

of the tire characteristics certainly holds for slip angles α_f with $|\alpha_{f0} - \alpha_f| < \varepsilon$. This extended linear tire model allows to investigate the vehicle dynamics at larger slip angles. It yields the traditional tire model (7) at $\alpha_{f0} = 0$. The term $f_{f0}(\alpha_{f0})$ is assumed constant. Hence, it does not play a role for stability analysis and will be neglected.

The cornering stiffness in dependency of the slip angle α_f is displayed in Figure 4 for various road surfaces. For small slip angles the cornering stiffnesses are independent of the road surface and remain almost at the same value until a certain magnitude of the slip angle is reached. Beyond this value the cornering stiffnesses decrease rapidly and may become negative* at large α_f.

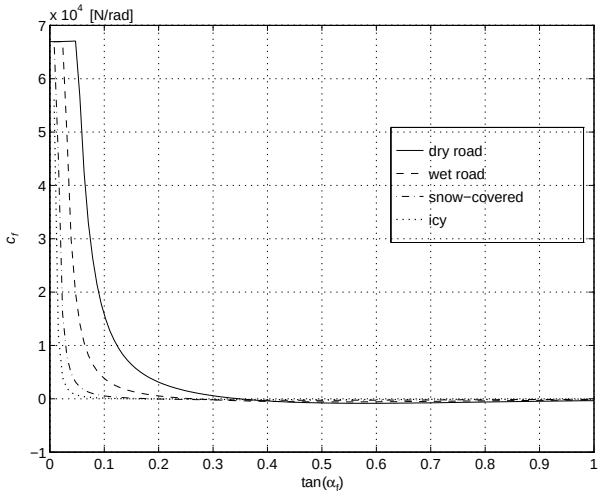

Figure 4: Cornering stiffness in dependency of the slip angle α_f at $v = 50\,\mathrm{km\,h^{-1}}$

In a first step the stability of the conventional vehicle is examined by inspecting the root locii of the vehicle for varying $c_f \in [-1000; 100000]$. Hereby, $c_r = 2c_f$† was assumed, the remaining vehicle parameters were set to typical data of a passenger car. The result is displayed in Figure 5. For positive c_f the vehicle is stable, for $c_f \leq 0$ the car is unstable with a double pole at the origin for $c_f = 0$ and one real pole in the right half plane for $c_f < 0$.

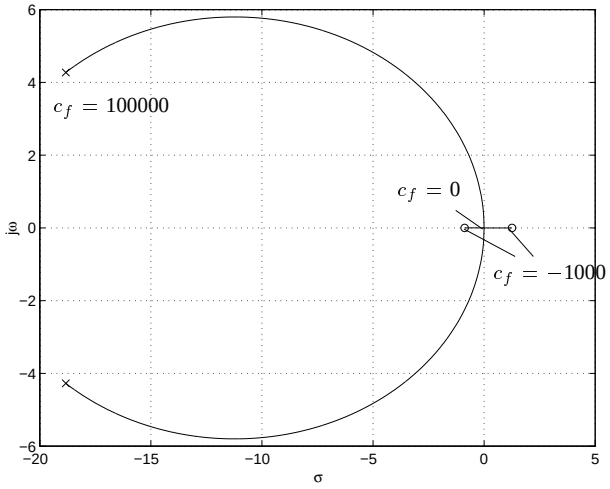

Figure 5: Root locii of a conventional vehicle for varying c_f at $v = 50\,\mathrm{km\,h^{-1}}$

The next question is how the active control law (2) influences the unstable driving situation at negative cornering stiffness compared to the conventional vehicle. Since the robust decoupling control law requires feedback of the yaw rate via an integrator the root locus of the transfer function $\frac{1}{s}\frac{r(s)}{\delta_f(s)}$ is illustrated in Figure 6. For positive feedback gains k, the degree of instability is even increased: The already unstable pole moves further to the right and the additional integrator pole also becomes unstable. The eigenvalues of the vehicle with robust decoupling ($k = 1$) are indicated by "$*$". The situation looks better for negative feedback: The unstable pole is moving towards the zero close to the origin and the stable pole "marries" the integrator pole and both become a complex pole pair which remains stable and converges towards the imaginary axis.

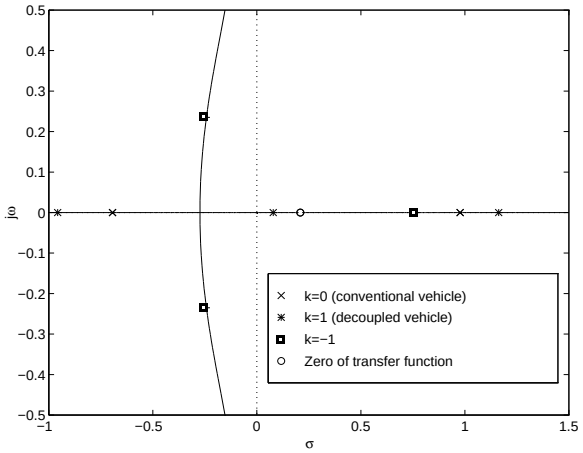

Figure 6: Root locus of the transfer function $\frac{1}{s}\frac{r(s)}{\delta_f(s)}$ for $c_f = -1000\,\mathrm{N\,rad^{-1}}$, $v = 50\,\mathrm{km\,h^{-1}}$

*In an attempt to capture somehow the different road conditions with the linear tire model a cornering stiffness $\mu \cdot c_{f0}$ is assumed, where μ denotes the road adhesion factor and c_{f0} is determined from the tire characteristics for dry road. There, the cornering stiffness may become small for icy road but never negative.

†Typically, the front cornering stiffness of the single track model includes the stiffness of the steering mechanism (steering column, gear, etc.). The inspection of several model data from different car manufacturers showed approximately the same relation between front and rear cornering stiffness.

These simple investigations revealed that robust decoupling increases the degree of instability when the cornering stiffness is negative. They also show that the cornering stiffness has crucial influence on the stability of the vehicle dynamics. The next section demonstrates how this parameter can be estimated.

3 Estimation of the cornering stiffness

Theorem The term

$$m \cdot \frac{\ell_r}{\ell_f + \ell_r} \cdot \frac{\dot{a}_f}{\dot{\delta}_f - \frac{a_f}{v} + r} =: \tilde{c}_f \tag{10}$$

is an estimate for the cornering stiffness c_f for $\dot{\delta}_f - \frac{a_f}{v} + r \neq 0$. ♢

Proof The above estimate can be calculated from the linearized vehicle equations (3), (4), and (6) assuming constant velocity. The calculation of the estimate is based on (8). It can be rewritten as

$$c_f(\alpha_f) = \frac{\mathrm{d}f_f(\alpha_f)}{\mathrm{d}\alpha_f} = \frac{\mathrm{d}f_f(\alpha_f)}{\mathrm{d}\alpha_f} \cdot \frac{\mathrm{d}t}{\mathrm{d}t} = \frac{\dot{f}_f}{\dot{\alpha}_f} \tag{11}$$

for $\mathrm{d}\alpha_f/\mathrm{d}t = \dot{\alpha}_f \neq 0$. The lateral tire force f_f is proportional to the lateral acceleration a_f at the front axle:

$$f_f = m_f \cdot a_f = m \cdot \frac{\ell_r}{\ell_f + \ell_r} a_f \tag{12}$$

The slip angle α_f can be expressed as

$$\alpha_f = \delta_f - \beta_f = \delta_f - \beta - \frac{\ell_f}{v} r \tag{13}$$

Its derivative is

$$\dot{\alpha}_f = \dot{\delta}_f - \dot{\beta} - \frac{\ell_f}{v} \dot{r} \tag{14}$$

Equation (4) with $\dot{v} = 0$ and $\beta^2 \approx 0$ yields

$$mv(\dot{\beta} + r) = f_y = m \cdot a = m \cdot \frac{\ell_f a_r + \ell_r a_f}{\ell_f + \ell_r} \tag{15}$$

where a is the lateral acceleration at the center of gravity. Equation (14) together with (15) and $\dot{r} = \frac{a_f - a_r}{\ell_f + \ell_r}$ results in

$$\dot{\alpha}_f = \dot{\delta}_f - \frac{a_f}{v} + r \tag{16}$$

The estimate for c_f is the quotient of the derivative of (12) and (16) yielding (10). ♢

To calculate the estimate for c_f measurements of the front steering angle δ_f, the yaw rate r and the lateral acceleration a_f at the front axle are necessary. The derivatives of the steering angle and the acceleration have to be calculated from the measured signals. Especially, the acceleration measurement is noisy and requires good filtering techniques, see e.g. [6].

The estimate is restricted to $\dot{\delta}_f - \frac{a_f}{v} + r \neq 0$. Under the assumption of the linearized single track model equations, this term is identical to $\dot{\alpha}_f$. It equals zero either in stationary driving situations or for cases when the tire slip angle has reached an extremum. In the first case it can be assumed that the cornering stiffness is identical to the last value computed in transient driving condition. In the second case no estimate can be calculated. However, this condition is restricted to some time points such that again the last computed value is used. For numerical issues the absolute value of $\dot{\delta}_f - \frac{a_f}{v} + r$ has to be greater than a threshold ε to compute a valid estimate. For a sampling time i the estimate $c^*_{f,i}$ is calculated as

$$c^*_{f,i} = \begin{cases} m \cdot \dfrac{\ell_r}{\ell_f + \ell_r} \cdot \dfrac{\dot{a}_{f,i}}{\dot{\delta}_{f,i} - \dfrac{a_{f,i}}{v_i} + r_i} \\ \qquad \text{for } |\dot{\delta}_{f,i} - \dfrac{a_{f,i}}{v_i} + r_i| > \varepsilon \\ c^*_{f,i-1} \text{ else} \end{cases} \tag{17}$$

A further assumption requires $\dot{v} = 0$, i.e. ride at constant velocity. This assumption will be violated heavily in the case of braking. Modern ABS systems, however, estimate the road adhesion during a braking action; this information could be used then in a driver information or control system.

To illustrate the quality of the estimate under optimal conditions, simulations of steering wheel input to a conventional vehicle were performed using the nonlinear single track model. The results are shown in Figure 7. Illustrated are the yaw rate r, the lateral acceleration at the front axle a_f, and the estimate of the cornering stiffness. The maneuver was performed for low road adhesion of $\mu = 0.1$ which corresponds to ice. Two different steering wheel step inputs were examined: The solid lines indicate a step of 10°, the dashed lines refer to a step input of 90°. While the first maneuver still is in the range of linear tire characteristics, the second maneuver exceeds this range and leeds to low cornering stiffness. The plot of the estimates of the cornering stiffnesses is accompanied by the plots of the actual cornering stiffnesses. In both cases they show good correspondence.

4 Application to active steering

The previous section showed that a reliable estimate for the cornering stiffness can be computed. A large cornering stiffness indicates that the tire characteristics is within the linear range and therefore the equations of the linearized single track model and the control laws obtained with this model are valid. For small or negative cornering stiffness the tire has reached its performance limits and the control laws derived for the linear single track model may even further destabilize the car. For this reason it is necessary to incorporate this important tire information into the control law.

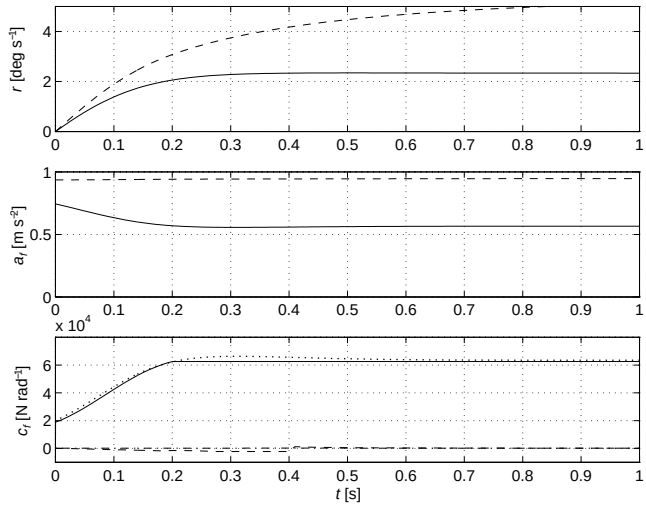

Figure 7: Simulation results for steering wheel step input at $v = 50\,\mathrm{km\,h^{-1}}$ (solid lines: $\delta_S = 10°$, dashed lines: $\delta_S = 90°$; a gear ratio of $i_s = 16$ was assumed for the simulations)

The root locus in Figure 6 shows that for negative cornering stiffness the degree of instability is reduced by negative feedback gain for the yaw rate. However, it is impossible to stabilize the vehicle in this driving condition with this controller. This could only be accomplished by a different controller structure which would require switching between the robust decoupling control law for positive cornering stiffness and the new controller structure for negative c_f. In view of reliability and safety requirements of the controlled car a switching controller structure is certainly not desirable. Furthermore, the vehicle rapidly looses controllability for small cornering stiffness, which can be be seen from the determinant of the controllability matrix

$$c_f^2 \frac{c_r(\ell_f + \ell_r)(J - \ell_f \ell_r m) + \ell_f^2 m^2 v^2}{J^2 m^2 v^2} \qquad (18)$$

which is zero for $c_f = 0$.

Summarizing the above suggests not to stabilize the car for small or negative cornering stiffness by adaptation of controller parameters or structure. A better approach is to imitate an experienced driver: he/she would decrease the steering wheel angle until the tire saturation region is left.

By means of control this can be accomplished by subtracting an angle $\tilde{\delta}_s$ from the driver commanded steering wheel angle. The angle to be subtracted has to grow constantly in magnitude until the cornering stiffness has reached a certain threshold or the front steering angle is completely reset to zero. The active control law is then

$$\begin{aligned} \delta_f &= i_s \cdot \delta_S - \tilde{\delta}_S + \delta_c \\ \dot{\delta}_c &= F(v) \cdot (i_s \cdot \delta_S - \tilde{\delta}_S) - r \end{aligned} \qquad (19)$$

with

$$\tilde{\delta}_S = \begin{cases} \operatorname{sign}\delta_S \cdot \min(|i_s \cdot \delta_S|, \tilde{\delta}_{S0} + k_c \int \mathrm{d}t) & \text{for } c_f^* < \tilde{c}_f \\ \operatorname{sign}\delta_S \cdot \max(0, \tilde{\delta}_{S0} - k_c \int \mathrm{d}t) & \text{else} \end{cases} \qquad (20)$$

where $\tilde{c}_f$ is the threshold value of the cornering stiffness which has to be undergone to force reduction of the driver commanded steering wheel angle and $\tilde{\delta}_{S0}$ is the integrator state when passing the threshold. Beyond this threshold linear tire characteristics is assumed, below this value the tire has reached or is about to reach tire saturation. The parameter k_c determines the velocity with which the additional angle $\tilde{\delta}_S$ grows. The integrator is restricted to $i_s \cdot \delta_s$ such that in the case of tire saturation at most the steering wheel angle can be compensated. Once the cornering stiffness has passed the threshold the additional angle returns to zero to guarantee an offset free steering wheel position. Note that a threshold value of $\tilde{c}_f = 0$ leads to maximum lateral force control.

The benefit of this additional feedforward control is investigated now in simulations. A typical maneuver which exceeds the linear tire range is aquaplaning. Stationary cornering on dry road at a velocity of $130\,\mathrm{km\,h^{-1}}$ with a stationary lateral acceleration of $6\,\mathrm{m\,s^{-2}}$ is assumed. At $t = 0.5\,\mathrm{s}$ the front tires hit a spot with low friction, for example an ice patch or water film. At $t = 1\,s$ it is returning to dry road. Fixed control is assumed, i.e. the steering wheel angle remains constant. The simulation results are displayed in Figure 8.

Due to the integrating control law the steering angle of the robustly decoupled vehicle is being increased dramatically, see Figure 8a). The robustly decoupled vehicle with additional feedforward (Figure 8b)) shows the desired "experienced driver behavior": the steering angle is reduced until a certain positive threshold value of the cornering stiffness is reached. After passing the water film the front steering angle returns very soon to the initial value, while it takes much more time in Figure 8a) to return to the initial value of δ_f. Furthermore, the lateral acceleration at the end of the water film builds up much softer compared to the vehicle without additional feedforward or to the conventional vehicle (Figure 8c)).

5 Conclusions

The major limitation of vehicle dynamics is due to nonlinear tire characteristics. In this paper, it was demonstrated how to estimate the cornering stiffness, an important tire parameter. The estimate could be used in conventional vehicles for an on-line warning of the driver. For vehicles with lateral control, for example active steering, this information can be used to be incorporated into the control law. As an example, an extension of the robustly decoupling control law by Ackermann was given and verified in simulations.

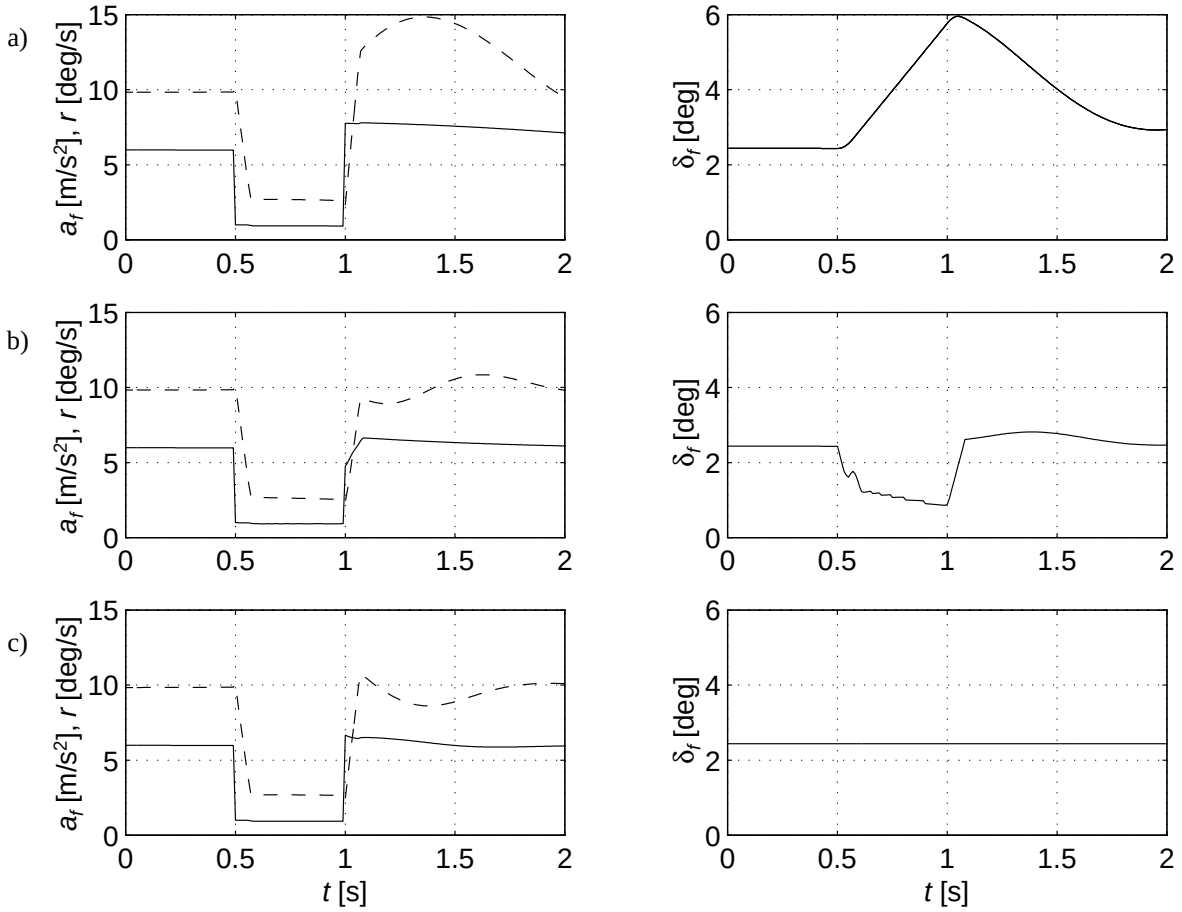

Figure 8: Aquaplaning maneuver: a) vehicle with robust decoupling, b) vehicle with extended robust decoupling, c) conventional vehicle (figures on the left: solid lines: lateral acceleration at front axle, dashed lines: yaw rate)

References

[1] J. Ackermann, "Yaw disturbance attenuation by robust decoupling of car steering," in *Proc. 13th IFAC World Congress*, vol. Q, (San Francisco), pp. 1–6, 1996.

[2] J. Ackermann, T. Bünte, W. Sienel, H. Jeebe, and K. Naab, "Driving safety by robust steering control," in *Proc. Int. Symposium on Advanced Vehicle Control*, (Aachen, Germany), 1996.

[3] W. Sienel, "Robust decoupling for active car steering holds for arbitrary dynamic tire characteristics," in *Proc. Third European Control Conference*, (Rom), 1995.

[4] H. Dugoff, P. Fancher, and L. Segel, "Tire performance characteristics affecting vehicle response to steering and braking control inputs," tech. rep., Highway Safety Research Institute (HSRI), University of Michigan, Ann Arbor, 1969. Final Report National Bureau of Standards Contract CST-460.

[5] J. Ackermann, A. Bartlett, D. Kaesbauer, W. Sienel, and R. Steinhauser, *Robust control: Systems with uncertain physical parameters.* London: Springer, 1993.

[6] F. Gustafsson, "A comparative study on change detection for some automotive applications," in *Proc. European Control Conference*, (Brussels, Belgium), 1997.